



Geophysical Research Letters

RESEARCH LETTER

10.1029/2020GL086955

Key Points:

- A new geothermal heat flux map for the continental Antarctica is presented
- Based on the latest seismic structure of Antarctica, the new map has improved resolution and reduced uncertainties
- New features of the map include high GHF in the Thwaites Glacial region and southern Transantarctic Mountains

Supporting Information:

- Supporting Information S1

Correspondence to:

W. Shen,
weisen.shen@stonybrook.edu

Citation:

Shen, W., Wiens, D., Lloyd, A., & Nyblade, A. (2020). A geothermal heat flux map of Antarctica empirically constrained by seismic structure. *Geophysical Research Letters*, 47, e2020GL086955. <https://doi.org/10.1029/2020GL086955>

Received 6 JAN 2020

Accepted 28 MAY 2020

Accepted article online 20 JUN 2020

A Geothermal Heat Flux Map of Antarctica Empirically Constrained by Seismic Structure

Weisen Shen¹ , Douglas A. Wiens² , Andrew J. Lloyd^{2,3} , and Andrew A. Nyblade⁴ 

¹Department of Geosciences, State University of New York at Stony Brook, Stony Brook, NY, USA, ²Department of Earth and Planetary Sciences, Washington University in St Louis, St. Louis, MO, USA, ³Now at Lamont-Doherty Earth Observatory, Columbia University, New York, NY, USA, ⁴Department of Geosciences, Pennsylvania State University, University Park, PA, USA

Abstract The geothermal heat flux (GHF) is an important boundary condition for modeling the movement of the Antarctic ice sheet but is difficult to measure systematically at a continental scale.

Earlier GHF maps suffer from low resolution and possibly biased assumptions in tectonism and crustal heat generation, resulting in significant uncertainty. We present a new GHF map for Antarctica constructed by empirically relating the upper mantle structure to known GHF in the continental United States. The new map, compared with previously seismologically determined one, has improved resolution and lower uncertainties. New features in this map include high GHF in the southern Transantarctic Mountains where warmer uppermost mantle is introduced by lithospheric removal and in the Thwaites Glacier region. Additionally, a modest GHF in the central West Antarctic Rift system near the Siple Coast and an absence of large-scale regions with GHF greater than 90 mW/m² are found.

Plain Language Summary The flow of the heat from Earth's interior into the ice sheet of Antarctica, or geothermal heat flux, has been poorly constrained but is important for understanding the movement of the ice sheet. In this study, we present a new map of the geothermal heat flux estimated from the latest studies of the seismic structure of Antarctica. This is accomplished by directly relating seismic wave speeds with heat flux for the continental United States, a place where many local heat flux measurements have been collected. The new map contains features that have not been reported before. For example, we find that more heat is coming out from the base of the southern Transantarctic Mountains, which is perhaps related to the missing thick and cold lithosphere beneath that region. We also report that part of West Antarctica may have lower geothermal heat flux than previously reported. The new map will help model the movement of the Antarctic ice sheet and predict its future.

1. Introduction

The geothermal heat flux (GHF) beneath ice sheets is an important boundary condition for ice dynamics, as it controls the basal melt of ice and thus strongly influences friction at the bed. Accurately measuring it for Antarctica is required for modeling of the development and future evolution of the its ice sheet and thus has important implications for global climate and sea-level change (Golledge et al., 2015; Parizek et al., 2003; Pattyn, 2010; Pollard et al., 2005). For West Antarctica, ice sheet modeling shows that an elevated GHF (e.g., ~100 mW/m²) due to a possible hot spot can produce significant basal melt locally (Seroussi et al., 2017). Observationally, near the Thwaites Glacier catchment, radar studies revealed presence of water at the base of the ice sheet, which was also related to the possible high GHF (Carter et al., 2009).

The importance of GHF, however, presents a strong contrast with the scarcity of local measurements due to inaccessibility and thick ice cover (Fretwell et al., 2013), as well as strong variability due to the complicated sub-ice hydrological system (e.g., Wright & Siegert, 2012). In West Antarctica, GHF values have been made at borehole sites (e.g., Byrd Station, Gow et al., 1968; McMurdo Sound, Schröder et al., 2011) and from the ice temperature profiles (e.g., Siple Dome, Engelhardt, 2004), and these values vary from 60 to more than 120 mW/m². A more extreme example is near the Whillans ice steam, where both modest (88 ± 7 mW/m², Begeman et al., 2017) and extremely high GHF values (~ 285 ± 80 mW/m², Fisher et al., 2015) have been reported. Study of the heat production determined by the geochemical composition of glacial rock clasts eroded from the continental interior suggests an average GHF of 48.0 ± 13.6 mW/m² for parts of the East

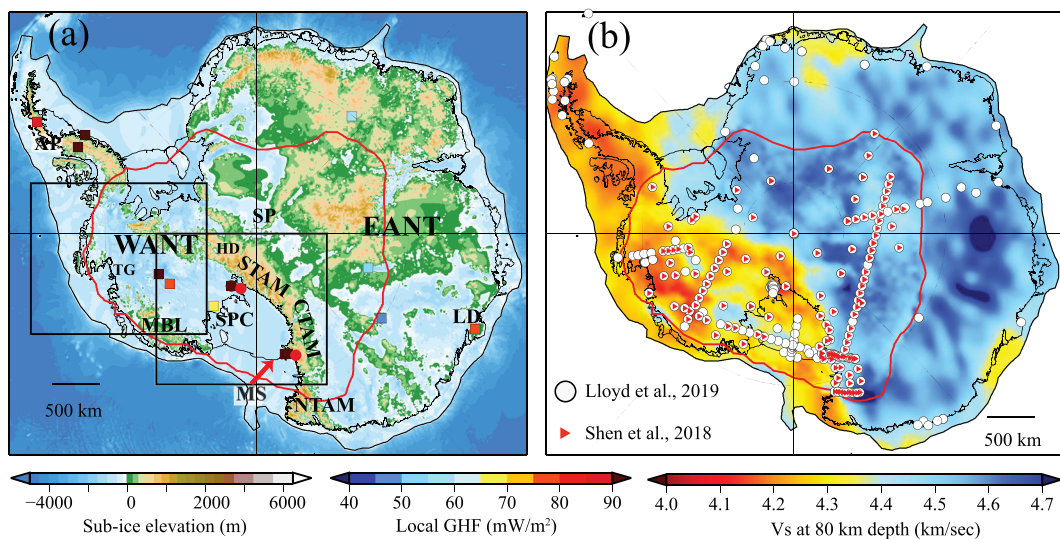


Figure 1. (a) Topographic features of Antarctica are marked on top of the sub-ice elevation map (Fretwell et al., 2013). EANT and WANT = East and West Antarctica; STAM, CTAM, NTAM = southern, central, and northern Transantarctic Mountains; MBL = Marie Byrd Land. Contour outside of the shore line marks the approximate extension of the continental Antarctica. Selected geographic locations such as the South Pole (SP), the Siple Coast (SPC), the Thwaites Glacier (TG), the McMurdo Sound (MS), the Law Dome (LD), the Herculus Dome (HD), and the Antarctic Peninsula (AP) are also marked by abbreviations; colored boxes show the local GHF measurements from ice sheet temperature profiles, while the colored circles represent the GHF from direct measurement. (b) A map view of Vs at 80 km beneath the surface of the solid Earth. The red contour highlights the boundary of the model of Shen, Wiens, Stern, et al. (2018) and Shen, Wiens, Anandakrishnan, et al. (2018) embedded in the model of Lloyd et al. (2019). Seismic stations are shown as red triangles and black circles by the two studies, respectively. The two boxes highlight the focus regions where blowup of the GHF maps is shown in Figure 5.

Antarctica craton (Goodge, 2018), but regions of high crustal heat production might produce locally elevated GHF estimates (e.g., Carson et al., 2014; Jordan et al., 2018; Mony et al., 2020). Surface geological mapping provides constraints on variations in crustal heat production, which is important for GHF estimates (Burton-Johnson et al., 2017), but can only be applied to limited areas where bedrock outcrops exist and have been mapped. Overall, these local, quasilocal, and regional estimates of GHF suggest significant variation of GHF across the continent but do not completely fulfill the needs of ice sheet dynamic modeling. Instead, a high-resolution map of GHF with uncertainties that covers the whole continent is required.

At a continental scale, geomagnetic methods provide estimates of the Curie depth, an isotherm of ~850 K corresponding to the change of the ferromagnetic properties. With proper conductive modeling in the magnetic crust, the Curie depth estimates provide constraints on the GHF for Antarctica (Fox-Maule et al., 2005; Martos et al., 2017 [F2005 and M2017 hereafter]), but this method requires assumptions in crustal heat generation and tectonic regionalization (i.e., tectonically active West vs. more stable East Antarctica [M2017]), introducing further potential sources for error. For instance, areas of East Antarctica just inboard from the southern Transantarctic Mountains (TAM) have been assumed to represent stable craton and thus have relatively low GHF in M2017 map, but recent seismic study revealed an absence of lithosphere resulting from lithospheric removal (Figure 1b; Shen, Wiens, Stern, et al., 2018), a mechanism that is capable to produce crustal volcanism and elevated GHF.

Seismological methods provide estimates of the lithospheric thermal structure based on the thermal sensitivity of seismic properties (i.e., shear velocity). Continental-scale GHF map can be produced through thermal modeling by converting uppermost mantle Vs to temperature profiles with assumptions about the thermal properties (An et al., 2015). The disadvantage of this method is that there are significant uncertainties associated with many parameters (Lösing et al., 2020), such as the temperature derivative of seismic velocity, and the temperature in the crust is difficult to determine from seismic velocity due to large and poorly constrained compositional variations (e.g., Haeger et al., 2019). Alternatively, one can empirically relate global GHF to lithospheric structures by comparison between Antarctica and other places with better

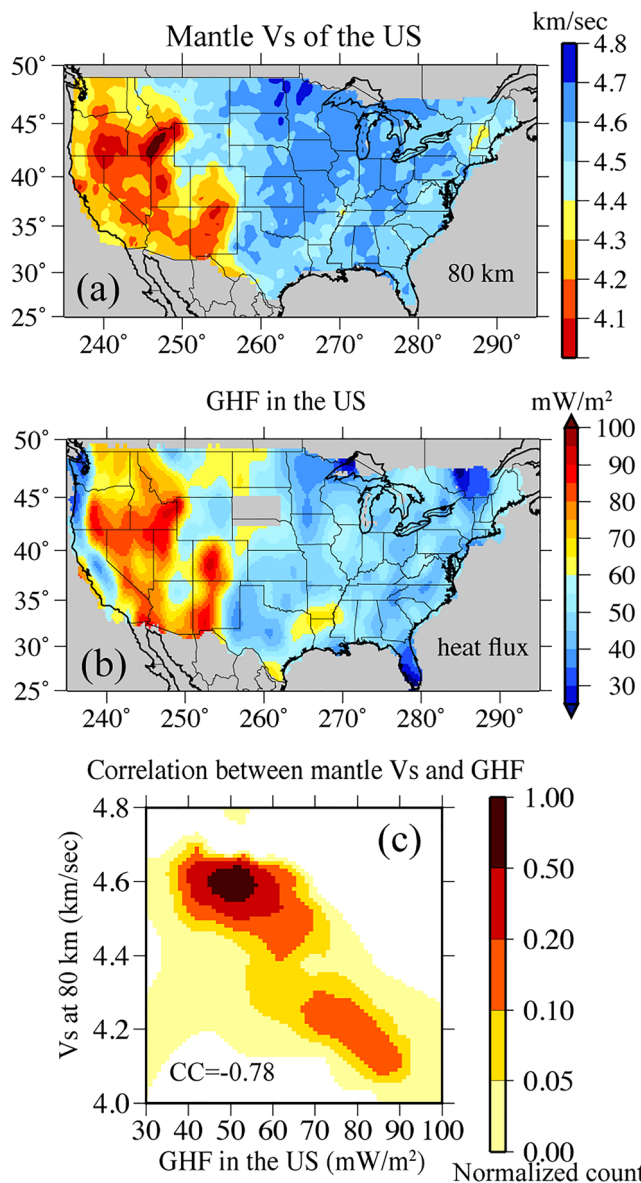


Figure 2. Illustration of the GHF determination method for a sample location (the South Pole) in Antarctica. (a) Mantle structure in the United States is shown by the map of shear velocity at 80 km depth (Shen & Ritzwoller, 2016). (b) Smoothed map of geothermal heat flux measured in the United States is shown in which the South Dakota hydrothermal anomaly has been removed. (c) Correlation between the mantle Vs and GHF values are shown by the normalized 2-D histogram.

Ritzwoller, 2016; Figure 2a) and GHF (Blackwell et al., 2011; Figure 2b). The continental U.S. GHF is highly correlated with the uppermost mantle shear wave velocity at 80 km (Figure 2c and Supporting Information S1) as well as other uppermost mantle depth range, further indicating that mantle seismic velocities can be used as a proxy of GHF: If the two regions in Antarctica and continental United States have similar upper mantle structure, the GHF values should also be similar. We note that the correlation is not strictly linear, and for a given mantle shear velocity, instead a single value, a distribution of GHF can be obtained, leading to the nonuniqueness in determining the GHF. This nonuniqueness is mostly due to factors such as crustal heat generation variations and local hydrological conditions, which should be considered as sources of uncertainties when the proxy is used. In this study, we use the width of the distribution to quantify this non-uniqueness rooted from the unknown crustal heat production and other factors.

measured GHF values. The later approach produced the first continental-scale GHF map for Antarctica (Shapiro & Ritzwoller, 2004, SR2004 hereafter), but it suffered from lower resolution of the seismic models and insufficient GHF measurements from global GHF maps.

In this paper, we present an empirically determined GHF map for continental Antarctica based on recent seismic velocity models for the Antarctic upper mantle. These models now have much higher resolution, as a result of taking advantage of more than 200 seismic stations in Antarctica deployed over the past 18 years (e.g., Shen, Wiens, Anandakrishnan, et al., 2018). Particularly, for each locality in Antarctica, we identify a structurally similar region (SSR) in the continental United States by comparing its uppermost mantle Vs with the continental U.S. model constructed by EarthScope/USArray data (Shen & Ritzwoller, 2016). This method overcomes many of the uncertainties associated with the thermal modeling method and also provides statistical measures of the confidence of the result.

2. Data and Methods

We use a seismic model for Antarctica that was developed by combining two recent models. In 2018, Shen et al. developed a high-resolution (~100 km) Vs model by incorporating both surface waves and receiver functions. This model has the greatest resolution in the crust and uppermost mantle and also has the advantage that it is constructed with the same methods used in the corresponding continental U.S. model (Shen & Ritzwoller, 2016). However, this method requires significant density of seismic stations, so the model is confined to the areas of the West and central Antarctica where most stations are located (Figure 1b). For the rest of the continent including the offshore continental shelf, we adopted a model that spans Antarctica and Southern Oceans that was constructed using a full waveform inversion technique, but which has somewhat lower resolution (Lloyd et al., 2019). These two models are quantitatively consistent with each other in the overlapping areas (the mean difference is -1.13 m/s, and standard deviation is ~ 74.09 m/s; for more details, see Supporting Information S1), allowing us to combine them into one complete 3-D model (Figure 1b).

The Antarctic seismic model is compared with seismic and GHF measurements of the continental United States to provide empirical estimates of Antarctic GHF. The continental United States provides an ideal comparison because it is well studied geophysically and it contains a wide range of geological provinces ranging from Archean craton to areas undergoing active tectonism and volcanism. In this study, we use the latest lithospheric shear wave velocity model constructed using USArray (Shen &

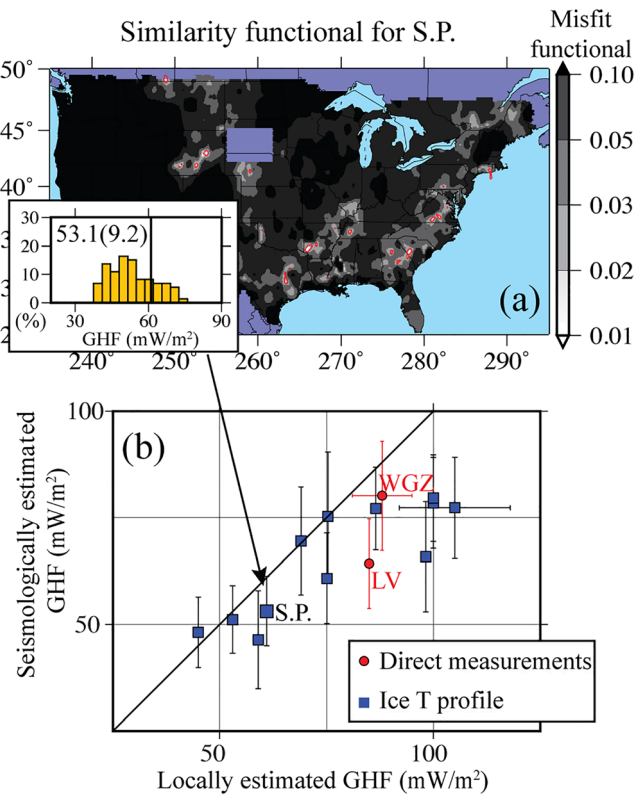


Figure 3. (a) Structurally similar regions (SSR) in the continental United States for the South Pole are marked by red contours on top of a map of the similarity functional. Inset: The histogram shows the corresponding GHF values. The in situ GHF estimate (Price et al., 2002, 61 mW/m²) is also marked. (b) Comparison of the estimated Antarctic GHF values from this study and in situ measurements (Supporting Information S5). Red circles show that the values are from ice sheet temperature profile, and squares mark the GHF values measured directly from the solid Earth (WGZ = Whillans Ice Stream Grounding Zone; LV = Lake Vida).

dently measured GHF values representing very localized GHF values, and their compatibility with large-scale tectonically induced GHF variations is often low as they contain the complex perturbations due to localized crustal heat generations, shallow hydrological circulations, and nonsteady-state convection in the lithosphere. But we still find that,

Figure 3 presents an example of this analysis for the South Pole (SP) where local GHF value is available from the ice sheet temperature profile (Price et al., 2002). For SP, we define an SSR in the continental United States, in which its uppermost mantle structure is the most similar to SP. In this process, we discretize the continental United States into $0.25^\circ \times 0.25^\circ$ grids and then identify the top 0.5% structurally similar grid points. These grid points span a total area of $200 \times 200 \text{ km}^2$, representing an averaged resolution of the tomographic models of the Antarctica. The SSR for SP is shown in Figure 3a, showing that SP's uppermost mantle structure is very similar to a number of places in the central and eastern United States. The distribution of the GHF values in this SSR allows us to estimate the GHF for SP: The weighted average of the distribution is a proxy for the GHF of SP (~53.1 mW/m²; Appendix), and the uncertainty is defined as the standard deviation of the distribution (9.2 mW/m²). This estimate is roughly compatible with the measurement from temperature profiles (61 mW/m², Price et al., 2002).

We note that the definition of SSR is empirical and based solely on the uppermost mantle Vs structure. The choice of 0.5% is made to balance the trade-off between bias and resolution: A smaller SSR leads to a narrower distribution of GHF for each point, but the mean is more likely to be biased. A greater SSR, however, would produce a smoothed GHF map and lower its resolution. Therefore, we conclude that the choice of the SSR area is subject to adjust when better lithosphere model of Antarctica is obtained, or other continents are used to calibrate. Furthermore, we note that factors such as crustal thickness are not part of the similarity calculation, because compared with uppermost mantle speed, crustal thickness is less correlated with observed GHF (Supporting Information S1; Lösing et al., 2020).

3. Results and Discussion

We apply the procedure to the entire Antarctic continent including the continental shelves and develop maps of the estimated GHF and associated uncertainties (Figure 4). There are a limited number of independent measurements made from temperature profiles from ice cores or sub-ice drilling, and their compatibility with large-scale tectonically induced GHF variations is often low as they contain the complex perturbations due to localized crustal heat generations, shallow hydrological circulations, and nonsteady-state convection in the lithosphere. But we still find that,

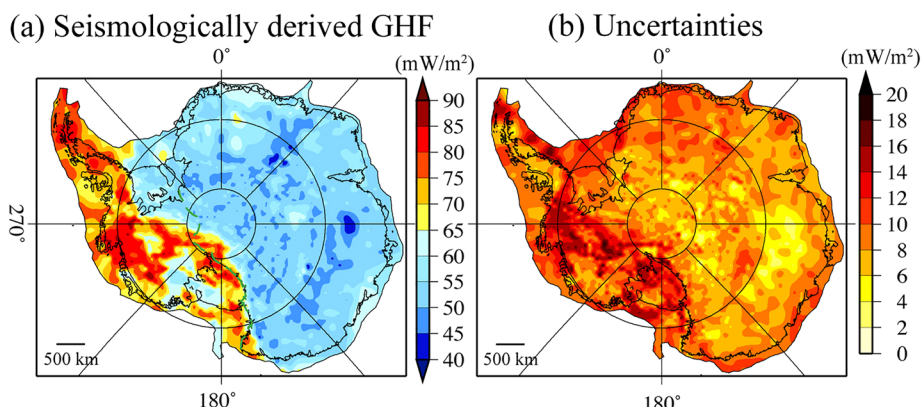


Figure 4. (a, b) Resulting GHF map and associated uncertainties for the continental Antarctica.

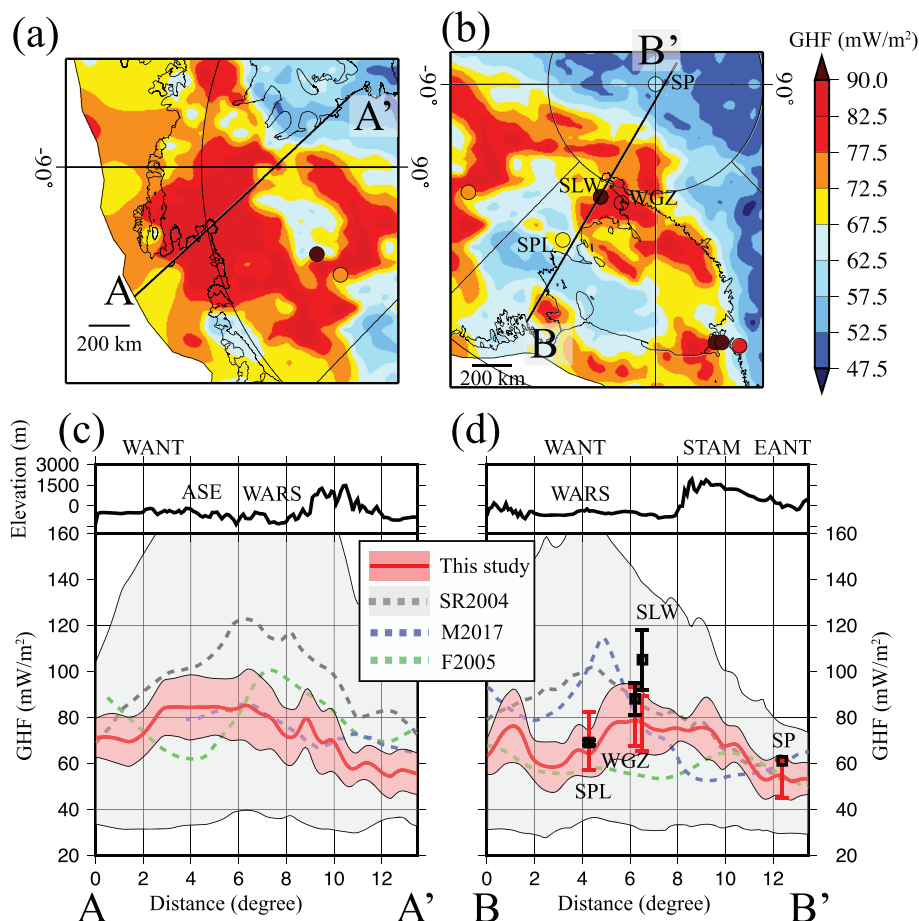


Figure 5. (a) GHF variations near the Amundsen Sea Coast (ASE, encompassing the Thwaites Glacier area) and Marie Byrd Land. Local measurements are shown as small circles. (b) Similar to (a), but for GHF variations near the central and southern Transantarctic Mountains and Siple Coast. (c, d) Estimated GHFs from this study together with uncertainties are shown as red line and pink corridors; seismically determined GHFs and uncertainties from global seismic structure (SR2004) are shown as gray dashed line and gray areas; green and blue dashed lines represent the geomagnetically determined GHFs from M2005 and M2017 maps, respectively. Black square and error bars highlight some nearby local GHF estimates: SPL = Siple Dome; SP = South Pole; SLW = Subglacial Lake Whillans; WGZ = Whillans Ice Stream Grounding Zone.

on average, the seismic estimates are similar to most of the localized values (Figure 3b and Supplementary Files), with some local values on the lower side (e.g., near the Whillans Ice Stream and McMurdo area, Morin et al., 2010; Risk & Hochstein, 1974). Two reasons contribute to some larger difference: (1) The temperature profile-determined GHF might be overestimated due to the additional frictional heating at the base of the ice sheet, and (2) the limited resolution ($\sim 100\text{--}200$ km) in the seismic model will not capture the small-scale variations in GHF along major tectonic boundaries (e.g., the TAM front.)

The results show an average continent-wide GHF of 59.7 mW/m^2 and uncertainty of 9.0 mW/m^2 . Notably, a dichotomy between East (averaged $\sim 52 \text{ mW/m}^2$) and West (averaged $\sim 80 \text{ mW/m}^2$) Antarctica shows up, consistent with earlier maps (SR2004; An et al., 2015). At smaller scales ($\sim 100\text{--}500$ km), features that have not been reported before can be further identified: First, instead of strictly following the TAM front ranges, the sharp boundary between high GHF East Antarctica and low GHF West Antarctica has a more complex geometry. Certain areas of East Antarctica exhibit high GHF ($>80 \text{ mW/m}^2$) such as the high plateau of the STAM and part of Northern Victoria Land (Figure 5), contrasting to the map based on the geomagnetic field. Second, high values in West Antarctica are found along the Peninsula, Amundsen Sea Coast encompassing the Thwaites Glacier, Marie Byrd Land, and along the TAM (Figures 5a and 5b). The low sub-ice topography

regions of the West Antarctic Rift system near the Siple Coast, however, show values \sim 55–75 mW/m 2 , consistent with its relatively long cooling time since the Cretaceous rifting (Siddoway, 2008), indicative of a thermal contraction of the lithosphere. These low values are substantially lower than some earlier continental maps but are consistent with that measured locally (e.g., at Siple Dome, the estimated GHF is 67.2 ± 12.7 mW/m 2 , compatible with the local GHF of $\sim 69 \pm 1$ mW/m 2 , Engelhardt, 2004). Third, instead being homogeneously low, the GHFs in East Antarctica show variations that have not been reported, due to the fact that the newly inferred seismic structure shows variable lithosphere thickness (Lloyd et al., 2019). Please note that near the SP, the estimated GHF is lower than the locally measured from the ice thermal profile. This might be related to the unrepresentativeness of the thermal profile to GHF but may also attribute to a potential crustal heat generation anomaly (e.g., Jordan et al., 2018). Finally, the new map does not show any regions of GHF greater than 90 mW/m 2 , in contrast to previous results suggesting very high heat flow in much of West Antarctica. For example, both SR2004 and M2017 show significant regions of West Antarctica with GHF greater than 110 mW/m 2 (Figures 5c and 5d and Supporting Information S1), and Schroeder et al. (2014) suggested that GHF was greater than 90 mW/m 2 throughout the entire Thwaites basin. The low estimates here suggest that the effect of GHF on ice dynamics will be significantly less than in some of the examples calculated in Seroussi et al. (2017).

The new map helps constrain the basal melt of the West Antarctic Ice Sheet. Three-dimensional ice-flow modeling shows that, given the homogeneous GHF of 60 mW/m 2 in the West Antarctica, basal melt exists in the areas of Thwaites Glacier as well as the ice streams feeding the Ross Ice Shelf (Seroussi et al., 2017). Additional modeling shows that once the basal temperature of melting is reached, basal melt rate further increases linearly with the GHF with a rate of \sim 0.3–0.4 mm/year/(mW/m 2). With the value of \sim 90 mW/m 2 for Thwaites Glacier, we estimate that an additional basal melt of \sim 10 mm/year will be obtained. In addition, at most subglacial lake sites ($>95\%$), the new map is either higher or close to \sim 55 mW/m 2 within uncertainties, allowing the active hydrological circulation system to emerge (Wright & Siegert, 2012). For Hercules Dome, we observe a GHF value of \sim 65 mW/m 2 due to the STAM lithospheric removal (Shen et al., 2018b), facilitating the formation of sub-ice lakes for this region as well.

Because of the smoothing length of Rayleigh waves (\sim 100 km) as well as the smoothing applied to the continental U.S. GHF map (\sim 50 km), this study estimates the regional average GHF over similar scales and thus lacks the resolution to resolve very small regions of high heat flow that may correspond to an individual volcanic edifice or small rift segment. Thus, isolated small-scale regions may show heat flow higher than estimated in this study. Another possible limitation is that this study is constrained by the range of tectonic environments present only in the continental United States. For example, the very low-GHF Archean cratonic lithosphere (Gard et al., 2019; Hasterok et al., 2019) may dominate some area of the East Antarctica but constitutes only a small portion of the contiguous United States. As a result, part of Archean Antarctica is represented by Proterozoic United States during the calibration and may lead us underestimate the lower bound of the GHF in Antarctica. To address this problem, more systematically GHF measurements and high-resolution seismic models in regions such as Australia and Africa are needed for further comparisons.

In summary, we present a new map of estimated GHF for continental Antarctica empirically determined from its upper mantle structure. Compared with earlier seismologically generated maps, the new map shows a better correlation with local observations. With the help of the high-resolution upper mantle structure, we are able to resolve the influence of tectonism such as the mantle lithosphere delamination of the STAM on the estimated GHF. This GHF map also provides new constraints for modeling of the ice sheet dynamics and evolution, which can potentially help estimate the melting rate of the West Antarctic Ice Sheet.

Data Availability Statement

Waveforms and metadata were accessed via the Incorporated Research Institutions for Seismology (IRIS) Data Management System, specifically the IRIS Data Management Center. At the time of submission, the model, uncertainties, and the 3-D model used are available online (<https://sites.google.com/view/weisen-research-products?authuser=0>). At the time of the publication, the resulting GHF maps (i.e., the mean and the standard deviation) are available via the U.S. Antarctic Program Data Center online (<https://cmr.earthdata.nasa.gov/search/concepts/C1833336298-SCIOPS.html>).

Acknowledgments

The authors thank the editor, and Tobias Staal and Derrick Hasterok for their insightful constructive review to the manuscript. This material is based upon work supported by the National Science Foundation under Grant PLR-1246712 (D. W.), PLR-1744883 (W. S., L. A., and D. W.), and PLR-1945856 (W. S. and D. W.). The IRIS DMS is funded through the National Science Foundation and specifically the GEO Directorate through the Instrumentation and Facilities Program of the National Science Foundation under Cooperative Agreement EAR-1063471.

References

- An, M., Wiens, D. A., Zhao, Y., Feng, M., Nyblade, A., Kanao, M., et al. (2015). Temperature, lithosphere–asthenosphere boundary, and heat flux beneath the Antarctic Plate inferred from seismic velocities. *Journal of Geophysical Research: Solid Earth*, *120*, 8720–8742. <https://doi.org/10.1002/2015JB011917>
- Begeman, C. B., Tulaczyk, S. M., & Fisher, A. T. (2017). Spatially variable geothermal heat flux in West Antarctica: Evidence and implications. *Geophysical Research Letters*, *44*, 9823–9832. <https://doi.org/10.1002/2017GL075579>
- Blackwell, D., Richards, M., Frone, Z., Batir, J., Ruzo, A., Dingwall, R., & Williams, M., 2011. Temperature-at-depth maps for the conterminous US and geothermal resource estimates (no. GRC1029452). Southern Methodist University Geothermal Laboratory, Dallas, TX (United States).
- Burton-Johnson, A., Halpin, J. A., Whittaker, J. M., Graham, F. S., & Watson, S. J. (2017). A new heat flux model for the Antarctic Peninsula incorporating spatially variable upper crustal radiogenic heat production. *Geophysical Research Letters*, *44*, 5436–5446. <https://doi.org/10.1002/2017GL073596>
- Carson, C. J., McLaren, S., Roberts, J. L., Boger, S. D., & Blankenship, D. D. (2014). Hot rocks in a cold place: high sub-glacial heat flow in East Antarctica. *Journal of the Geological Society*, *171*(1), 9–12.
- Carter, S. P., Blankenship, D. D., Young, D. A., & Holt, J. W. (2009). Using radar-sounding data to identify the distribution and sources of subglacial water: Application to Dome C, East Antarctica. *Journal of Glaciology*, *55*(194), 1025–1040. <https://doi.org/10.3189/002214309790794931>
- Engelhardt, H. (2004). Ice temperature and high geothermal flux at Siple Dome, West Antarctica, from borehole measurements. *Journal of Glaciology*, *50*(169), 251–256. <https://doi.org/10.3189/172756504781830105>
- Fisher, A. T., Mankoff, K. D., Tulaczyk, S. M., Tyler, S. W., & Foley, N. (2015). High geothermal heat flux measured below the West Antarctic Ice Sheet. *Science Advances*, *1*(6), e1500093. <https://doi.org/10.1126/sciadv.1500093>
- Fox-Maule, C., Purucker, M. E., Olsen, N., & Mosegaard, K. (2005). Heat flux anomalies in Antarctica revealed by satellite magnetic data. *Science*, *309*(5733), 464–467. <https://doi.org/10.1126/science.1106888>
- Fretwell, P., Pritchard, H.D., Vaughan, D.G., Bamber, J.L., Barrand, N.E., Bell, R., et al. (2013). Bedmap2: improved ice bed, surface and thickness datasets for Antarctica.
- Gard, M., Hasterok, D., Hand, M., & Cox, G. (2019). Variations in continental heat production from 4 Ga to the present: Evidence from geochemical data. *Lithos*, *342*, 391–406. <https://doi.org/10.1016/j.lithos.2019.05.034>
- Golledge, N. R., Kowalewski, D. E., Naish, T. R., Levy, R. H., Fogwill, C. J., & Gasson, E. G. (2015). The multi-millennial Antarctic commitment to future sea-level rise. *Nature*, *526*(7573), 421–425. <https://doi.org/10.1038/nature15706>
- Goodge, J. W. (2018). Crustal heat production and estimate of terrestrial heat flow in central East Antarctica, with implications for thermal input to the East Antarctic ice sheet. *The Cryosphere*, *12*(2), 491–504. <https://doi.org/10.5194/tc-12-491-2018>
- Gow, A. J., Ueda, H. T., & Garfield, D. E. (1968). Antarctic ice sheet: Preliminary results of first core hole to bedrock. *Science*, *161*(3845), 1011–1013. <https://doi.org/10.1126/science.161.3845.1011>
- Haeger, C., Kaban, M. K., Tesauro, M., Petrunin, A. G., & Mooney, W. D. (2019). 3-D density, thermal, and compositional model of the Antarctic lithosphere and implications for its evolution. *Geochemistry, Geophysics, Geosystems*, *20*, 688–707. <https://doi.org/10.1029/2018GC008033>
- Hasterok, D., Gard, M., Cox, G., & Hand, M. (2019). A 4 Ga record of granitic heat production: Implications for geodynamic evolution and crustal composition of the early Earth. *Precambrian Research*, *331*, 105375. <https://doi.org/10.1016/j.precamres.2019.105375>
- Jordan, T. A., Martin, C., Ferraccioli, F., Matsuoka, K., Corr, H., Forsberg, R., et al. (2018). Anomalously high geothermal flux near the South Pole. *Scientific Reports*, *8*(1), 1–8.
- Lloyd, A. J., Wiens, D. A., Zhu, H., Tromp, J., Nyblade, A. A., Aster, R. C., et al. (2019). Seismic structure of the Antarctic upper mantle based on adjoint tomography. *Journal of Geophysical Research: Solid Earth*, *125*, 2019JB017823. <https://doi.org/10.1029/2019JB017823>
- Lösing, M., Ebbing, J., & Szwilus, W. (2020). Geothermal heat flux in Antarctica: Assessing models and observations by Bayesian inversion. *Frontiers in Earth Science*, *8*, 105. <https://doi.org/10.3389/feart.2020.00105>
- Martos, Y. M., Catalán, M., Jordan, T. A., Golynsky, A., Golynsky, D., Eagles, G., & Vaughan, D. G. (2017). Heat flux distribution of Antarctica unveiled. *Geophysical Research Letters*, *44*, 11,417–11,426. <https://doi.org/10.1002/2017GL075609>
- Mony, L., Roberts, J. L., & Halpin, J. A. (2020). Inferring geothermal heat flux from an ice-borehole temperature profile at Law Dome, East Antarctica. *Journal of Glaciology*, *66*(257), 509–519. <https://doi.org/10.1017/jog.2020.27>
- Morin, R. H., Williams, T., Henrys, S. A., Magens, D., Niessen, F., & Hansaraj, D. (2010). Heat flow and hydrologic characteristics at the AND-1B borehole, ANDRILL McMurdo Ice Shelf Project, Antarctica. *Geosphere*, *6*(4), 370–378. <https://doi.org/10.1130/GES00512.1>
- Parizek, B. R., Alley, R. B., & Hulbe, C. L. (2003). Subglacial thermal balance permits ongoing grounding-line retreat along the Siple Coast of West Antarctica. *Annals of Glaciology*, *36*, 251–256. <https://doi.org/10.3189/172756403781816167>
- Pattyn, F. (2010). Antarctic subglacial conditions inferred from a hybrid ice sheet/ice stream model. *Earth and Planetary Science Letters*, *295*(3–4), 451–461. <https://doi.org/10.1016/j.epsl.2010.04.025>
- Pollard, D., DeConto, R. M., & Nyblade, A. A. (2005). Sensitivity of Cenozoic Antarctic ice sheet variations to geothermal heat flux. *Global and Planetary Change*, *49*(1–2), 63–74. <https://doi.org/10.1016/j.gloplacha.2005.05.003>
- Price, P. B., Nagornov, O. V., Bay, R., Chirkin, D., He, Y., Miocinovic, P., et al. (2002). Temperature profile for glacial ice at the South Pole: Implications for life in a nearby subglacial lake. *Proceedings of the National Academy of Sciences*, *99*(12), 7844–7847. <https://doi.org/10.1073/pnas.082238999>
- Risk, G. F., & Hochstein, M. P. (1974). Heat flow at arrival heights, Ross Island, Antarctica. *New Zealand Journal of Geology and Geophysics*, *17*(3), 629–644. <https://doi.org/10.1080/00288306.1973.10421586>
- Schröder, D., Heinemann, G., & Willmes, S. (2011). The impact of a thermodynamic sea-ice module in the COSMO numerical weather prediction model on simulations for the Laptev Sea, Siberian Arctic. *Polar Research*, *30*(1), 6334. <https://doi.org/10.3402/polar.v30i0.6334>
- Schroeder, D. M., Blankenship, D. D., Young, D. A., & Quartini, E. (2014). Evidence for elevated and spatially variable geothermal flux beneath the West Antarctic Ice Sheet. *Proceedings of the National Academy of Sciences*, *111*(25), 9070–9072. <https://doi.org/10.1073/pnas.1405184111>
- Seroussi, H., Ivins, E. R., Wiens, D. A., & Bondzio, J. (2017). Influence of a West Antarctic mantle plume on ice sheet basal conditions. *Journal of Geophysical Research: Solid Earth*, *122*, 7127–7155. <https://doi.org/10.1002/2017JB014423>
- Shapiro, N. M., & Ritzwoller, M. H. (2004). Inferring surface heat flux distributions guided by a global seismic model: Particular application to Antarctica. *Earth and Planetary Science Letters*, *223*(1–2), 213–224. <https://doi.org/10.1016/j.epsl.2004.04.011>

- Shen, W., & Ritzwoller, M. H. (2016). Crustal and uppermost mantle structure beneath the United States. *Journal of Geophysical Research: Solid Earth*, 121, 4306–4342. <https://doi.org/10.1002/2016JB012887>
- Shen, W., Wiens, D. A., Anandakrishnan, S., Aster, R. C., Gerstoft, P., Bromirski, P. D., et al. (2018). The crust and upper mantle structure of central and West Antarctica from Bayesian inversion of Rayleigh wave and receiver functions. *Journal of Geophysical Research: Solid Earth*, 123, 7824–7849. <https://doi.org/10.1029/2017JB015346>
- Shen, W., Wiens, D. A., Stern, T., Anandakrishnan, S., Aster, R. C., Dalziel, I., et al. (2018). Seismic evidence for lithospheric foundering beneath the southern Transantarctic Mountains, Antarctica. *Geology*, 46(1), 71–74.
- Siddoway, C. S. (2008). Tectonics of the West Antarctic Rift System: New light on the history and dynamics of distributed intracontinental extension. In *Antarctica: A keystone in a changing world*, (pp. 91–114). Washington, D. C: Natl. Acad. Press.
- Wright, A., & Siegert, M. (2012). A fourth inventory of Antarctic subglacial lakes. *Antarctic Science*, 24(6), 659–664. <https://doi.org/10.1017/S095410201200048X>

References From the Supporting Information

- Clow, G. D., Cuffey, K. M., & Waddington, E. D. (2012). High heat-flow beneath the central portion of the West Antarctic Ice Sheet. Abstract C31A-0577 Presented at the 2012 AGU Fall Meeting, San Francisco, CA.
- Dahl-Jensen, D., Morgan, V. I., & Elcheikh, A. (1999). Monte Carlo inverse modelling of the Law Dome (Antarctica) temperature profile. *Annals of Glaciology*, 29, 145–150. <https://doi.org/10.3189/172756499781821102>
- Decker, E. R., & Bucher, G. J. (1982). Geothermal studies in the Ross Island-Dry Valley region. *Antarct Geosci*, 4, 887–894.
- Dmitriev, A. N., Bolshunov, A. V., & Podoliak, A. V. (2016). Assessment of ice borehole temperature conditions at interface with subglacial Lake Vostok (Antarctica). *International Journal of Applied Engineering Research*, 11(11), 7230–7233.
- Gosnold, W. D. (1990). Heat flow in the Great Plains of the United States. *Journal of Geophysical Research*, 95(B1), 353–374. <https://doi.org/10.1029/JB095iB01p00353>
- Hasterok, D. (2010). Thermal state of the oceanic and continental lithosphere (Doctoral dissertation, PhD Thesis, University of Utah).
- Hondoh, T., Shoji, H., Watanabe, O., Salamatian, A. N., & Lipenkov, V. Y. (2002). Depth-age and temperature prediction at Dome Fuji station, East Antarctica. *Annals of Glaciology*, 35, 384–390. <https://doi.org/10.3189/172756402781817013>
- Nicholls, K. W., & Paren, J. G. (1993). Extending the Antarctic meteorological record using ice-sheet temperature profiles. *Journal of Climate*, 6(1), 141–150. [https://doi.org/10.1175/1520-0442\(1993\)006<0141:ETAMRU>2.0.CO;2](https://doi.org/10.1175/1520-0442(1993)006<0141:ETAMRU>2.0.CO;2)
- Ritz, C., Lefebvre, E., Dahl Jensen, D., Johnsen, S., & Sheldon, S. (2010). Temperature profile measurement in the EPICA Dome C borehole, EPICA Meeting 2010.
- Salamatian, A. N., Lipenkov, V. Y., Barkov, N. I., Jouzel, J., Petit, J. R., & Raynaud, D. (1998). Ice core age dating and paleothermometer calibration based on isotope and temperature profiles from deep boreholes at Vostok Station (East Antarctica). *Journal of Geophysical Research*, 103(D8), 8963–8977. <https://doi.org/10.1029/97JD02253>
- Zagorodnov, V., Nagornov, O., Scambos, T. A., Muto, A., Mosley-Thompson, E., Pettit, E. C., & Tyuflin, S. (2012). Borehole temperatures reveal details of 20th century warming at Bruce Plateau, Antarctic Peninsula. *The Cryosphere*, 6(3), 675–686. <https://doi.org/10.5194/tc-6-675-2012>